Structural and hyperfine characterization of σ-phase Fe-Mo alloys

J. Cieslak,* S. M. Dubiel, J. Przewoznik, and J. Tobola
AGH University of Science and Technology, Faculty of Physics and Applied Computer Science, al. Mickiewicza 30, 30-059 Krakow, Poland
(Dated: January 25, 2013)

A series of nine samples of σ-$Fe_{100-x}Mo_x$ with $44 \leq x \leq 57$ were synthesized by a sintering method. The samples were investigated experimentally and theoretically. Using X-ray diffraction techniques structural parameters such as lattice constants, atomic positions within the unit cell and populations of atoms over five different sublattices were determined. An information on charge-densities and electric field gradients at particular lattice sites was obtained by application of the Korringa-Kohn-Rostoker (KKR) method for electronic structure calculations. Hyperfine quantities calculated with KKR were successfully applied to analyze Mössbauer spectra measured at room temperature.

PACS numbers: 33.45.+x, 61.05.cp, 61.43.-j, 71.20.-b, 71.20.Be, 71.23.-k, 74.20.Pq, 75.50.Bb, 76.80.+y

I. INTRODUCTION

A σ-phase (space group $P4_2/mnm$, 30 atoms per unit cell), which belongs to a class of the so-called Frank-Kasper phases[1] characterized by a high coordination numbers (CN=12-15, for σ) can be formed in alloy systems by a solid state reaction at elevated temperatures. About 50 examples of σ were up-to-now found in such binary systems, including the Fe-Mo one. A possibility of occurrence of the σ-phase in Fe-Mo was first revealed in 1949 by Goldschmidt[2]. Studying a ternary system of Fe-Cr-Mo he had identified a new phase stable in the temperature interval of 1180 - 1540 °C. The phase had some similarities to the already-known σ-phase in Fe-Cr. Its crystallographic structure and parameters were definitely identified five years later[3]. Wilson was the first who determined the lattice parameters and distribution of atoms over the five sublattices for σ-$Fe_{50}Mo_{50}$ sample[4]. Further investigations depicting the structure and sites occupancy by Fe and Mo atoms were continued by other investigators, too[5,6]. Heijwegen determined borders for the existence of the σ-phase in the Fe-Mo system[7]. Finaly, the phase diagram which is regarded as the most actual was proposed by Guillermert[8].

In the Fe-Mo system, the σ-phase is one of three Frank-Kasper phases that can occur in that system. The other two ones are represented by μ (16 atoms per unit cell), and R (54 atoms per unit cell). They have different compositions and can be formed in different ranges of temperature than σ[9,10]. In the available literature, there is little information relevant to physical properties of the σ-phase in Fe-Mo. Even the data on its crystallographic structure in the whole concentration range of its occurrence is not complete. In these circumstances systematic studies aimed at filling this gap are justified, all the more so such studies have been recently carried out for this phase in Fe-Cr and Fe-V systems[11]. A comparison of corresponding data obtained for different binary alloy systems containing iron, Fe-X, where the σ-phase can be formed, is of interest *per se*, and, additionally, it may contribute to a better understanding of its formation mechanism. The konowledge of the letter is of a great importance in the light of a detrimental effect of a σ-phase presence in stainless steels used in various branches of industry as valuable construction materials. In this paper results of a systematic study of the lattice parameters, sites occupancies, Fe-site charge-densities and electric field gradients obtained using various experimental tools viz. X-ray diffraction (XRD) and Mössbauer spectroscopy (MS), as well as electronic structure calculations (KKR method) are presented in the whole concentration range of the

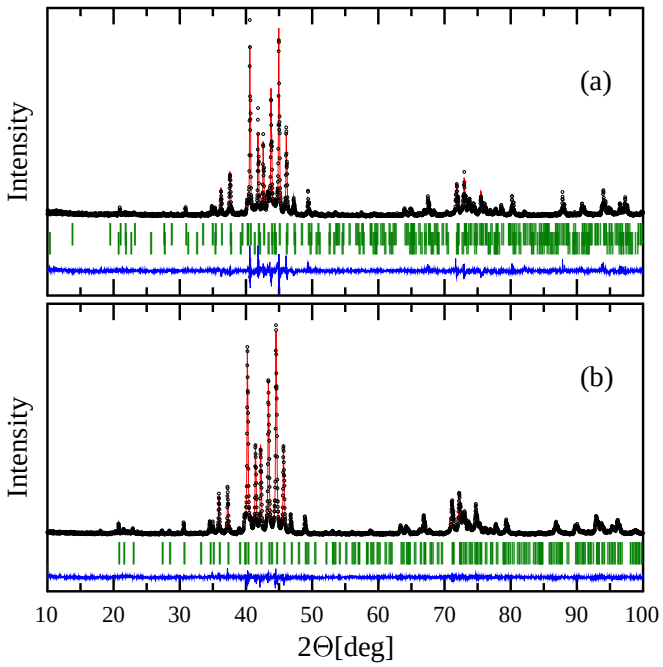

FIG. 1: (Online color) Parts of of selected fitted X-ray diffractograms recorded at 294K on the σ-phase sample of (a) $Fe_{55}Mo_{45}$ and (b) $Fe_{45}Mo_{55}$. The solid line stays for the best-fit obtained with the procedure described in the text. Peak positions for μ and σ (a) as well as for pure σ-phase (b) are indicated. A difference diffractograms are shown, too.

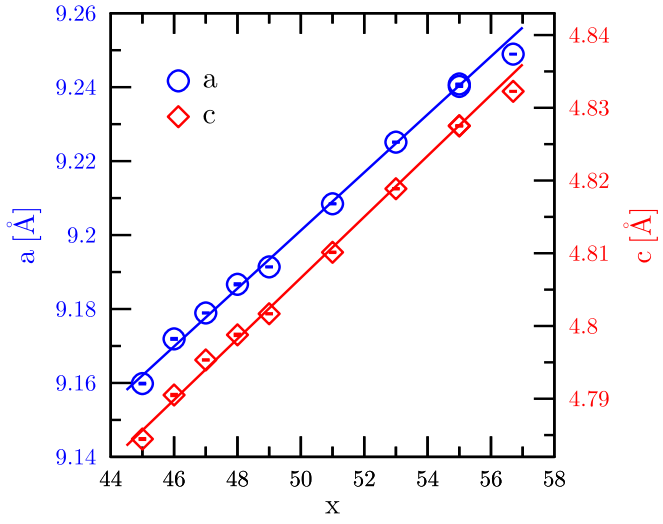

FIG. 2: (Online color) Dependence of the lattice parameters a (circles, blue) and c (diamonds, red) on Mo-content, x, as determined from the X-ray diffractograms recorded at 294K.

σ-phase existence in the investigated alloys.

II. EXPERIMENTAL

It was not possible to obtain samples in a pure σ-FeMo alloys by using the procedure that was previously successfully applied in the case of Fe-Cr and Fe-V alloys i.e. an isothermal annealing of ingots obtained by melting constituents[11]. The Fe-Mo ingots treated in that way were always two-phase, the second phase being μ. Successful was, however, a procedure described by Bergman[3] viz. a sintering. For that purpose, powders of elemental Fe (99.9at%) and Mo (99.95at%) were mixed together in adequate proportions. Next, 2 g tablets for each composition were fabricated by pressing the mixtures. The tablets were subsequently isothermally annealed at 1430° C during 6 hours, and afterwords quenched into liquid nitrogen. For XRD and Mössbauer spectroscopic measurements, both carried out at room temperature (RT = 294K), the pellets were attrited into powder in an agate mortar. Altogether nine samples with the following nominal concentration of Mo: 44, 45, 47, 48, 49, 51, 53, 55 and 57 at% were prepared. Based on the XRD patterns, an example of which is shown in Fig. 1, it was found that all samples except two with the lowest Mo content, and one with the highest content of Mo were single-phase, namely σ. The samples containing nominally 44 and 45 at% Mo had some admixture of μ-phase (Fig. 1a), and the most Mo-concentrated sample contained $\sim$ 4.2wt% of undissolved Mo-rich, *bcc* Fe-Mo phase. In the latter case the content of Mo in the σ-phase was estimated as equal to 56.7 at%.

III. RESULTS

The powder XRD patterns were collected at RT with a D5000 Siemens diffractometer (using Cu K-α radiation and a graphite secondary monochromator) from 10° to 140° in steps of 0.02° in 2θ. Data were analyzed by the Rietveld method as implemented in the FULLPROF program[12] with 22 free parameters: 6 of them were related to a background and positions of lines, 10 parameters represented sites occupancies and atomic positions in the unit cell. Remaining 6 parameters described line widths, lattice constants and Debye-Waller factors. The analysis yielded values of the lattice constants, a and c (Fig. 2, Table 1), atomic positions (Table 2), as well as occupancies of the sublattices (Fig. 3). Concerning the lattice constants, as clearly evidenced in Fig. 2, they exhibit a linear dependence on the Mo content, x. Yet, the ratio $c/a = 0.52233(2)$ is rather x-independent. For comparison, Bergman found the value of 0.5237 for this ratio[3]. The values of the lattice constants given in the literature[3,4,13] are in line with ours. This can be taken as indication that the nominal compositions of our samples can be regarded as very close to the real ones. Also the atomic positions found in our analysis agree within error limits with those known from the literature[3,13]. As far as the occupancy of the lattice sites is concerned, the analysis of the XRD patterns gave evidence that sites A and D were exclusively populated by Fe atoms, which is slightly different than in the case of the σ-phase in Fe-Cr and Fe-V systems where the population of Fe atoms at these sites was lying within 80-90% range[14]. The remaining three sites were found to be occupied by both Fe and Mo atoms, the former being in minority. However, the actual occupancy is concentration dependent and it decreases linearly with x at a rate characteristic of a given site. These results agree qualitatively with those reported earlier[4,13].

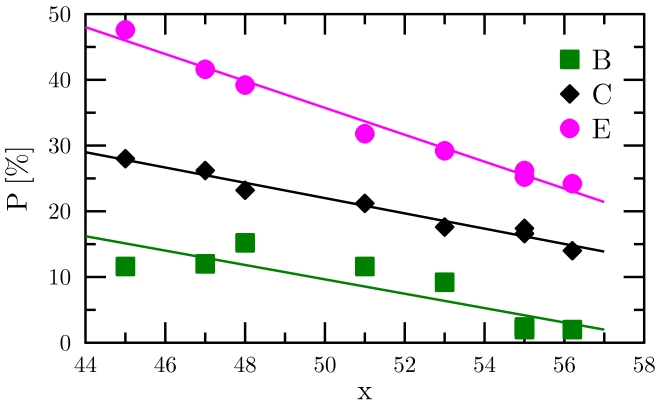

FIG. 3: (Online color) Probability of finding Fe atoms at different lattice sites in the σ-$Fe_{100-x}Mo_x$ compounds, P, versus Mo concentration, x. Solid lines stay for the linear fits to the data

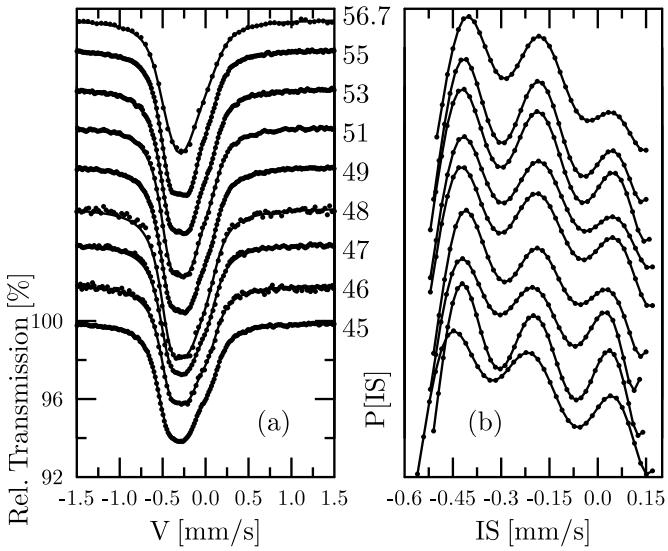

FIG. 4: (a) ^{57}Fe Mössbauer spectra recorded on a series of σ-$Fe_{100-x}Mo_x$ samples at 294K and labeled with the corresponding x-values. The solid lines are the best-fit to the experimental data. The derived isomer shift distribution curves, shown in the same sequence as the spectra, are indicated in (b).

^{57}Fe-site Mössbauer spectra, shown in Fig. 4a, were recorded in a transmission geometry using a standard equipment and Co/Rh source for the 14.4 keV gamma-radiation. No traces of magnetism at RT were found in all the spectra recorded at RT. Despite it is known from the XRD experiments that Fe atoms are present at all five sublattices, which means that each spectrum should be composed of at least five subspectra. However, an unique analysis of the measured spectra in terms of five components that could be associated with the five sublattices is not possible due to a lack of a well-defined structure of them. Instead, one can analyze them in terms of an isomer shift distribution, ISD, as explained elsewhere[15]. The ISD-curves obtained as a result of such analysis are presented in Fig. 4b. By integration of these curves, average values of the isomer shift, $\langle IS\rangle$, were obtained (Table 1). The dependence of the latter on the Mo content, x, is illustrated in Fig. 5. It is clear than an increase of x results in a linear decrease of $\langle IS\rangle$ for all samples, except for those with the lowest x-values. The departure in the latter case is likely due to the fact that these two samples had some small admixture of the μ phase. The decrease of $\langle IS\rangle$ (increase of the Fe-site charge-density) with x is rather weak, as it is equal to 0.0017 mm/s per at%. For comparison, in the case of the σ-FeV alloys, the rate of $\langle IS\rangle$ decrease was almost two times higher[16].

A lack of a well-resolved structure of the spectra did not allow to decompose them uniquely into the subspectra corresponding to the five sublattices, hence to determine charge-densities and electric field gradients characteristic of these sublattices. However, as demonstrated elsewhere[16,17], a knowledge of these two spectral quantities can be obtained with the help of electronic structure calculations. In the present case, the KKR calculations were carried out for 23 unit cells with different configurations of Fe and Mo atoms on the sublattices A, B, C, D and E, keeping experimental lattice constants in all cases. The configurations were chosen according to the following two criteria: (1) the probability of finding an Fe atom on a given site was as close as possible to the one found experimentally for σ-$Fe_{56}Mo_{44}$, and (2) each possible number of Fe atoms being the nearest-neighbors for a given lattice site, NN_{Fe}, has been taken into account.

TABLE I: Lattice constants (in Å), a and c as well as the average isomer shift,$\langle IS\rangle$, (in mm/s, relative to the Co/Rh source), for all investigated σ-$Fe_{100-x}Mo_x$ samples.

x	a	c	$\langle IS\rangle$
45.	9.1598(2)	4.7844(1)	-0.242
46.	9.1719(2)	4.7905(1)	-0.235
47.	9.1789(1)	4.7953(1)	-0.234
48.	9.1866(2)	4.7987(1)	-0.236
49.	9.1913(1)	4.8016(1)	-0.236
51.	9.2084(1)	4.8101(1)	-0.240
53.	9.2251(1)	4.8188(1)	-0.242
55.	9.2402(1)	4.8275(1)	-0.248
56.7	9.2489(1)	4.8322(1)	-0.252

The charge and spin self-consistent Korringa-Kohn-Rostoker Greens function method[18–20] was here used to calculate the electronic structure of the Fe-Mo σ-phase. The crystal potential of the muffin-tin form was constructed within the LDA framework, using the Barth-Hedin formula for the exchange-correlation part. The experimental values of lattice constants and atomic positions were used here. For fully converged crystal potentials electronic density of states (DOS), total, site-composed and l-decomposed DOS (with $l_{max} = 2$ for both types of atoms) were derived. Fully converged results were obtained for $\sim$ 120 special **k**-points grid in the irreducible part of Brillouin zone. DOS were computed using the tetrahedron **k** space integration technique and $\sim$ 700 small tetrahedrons[21]. More details can be found

TABLE II: Atomic crystallographic positions, x, y, z, for the five lattice sites of the Fe-Mo σ-phase. Since the values were weakly composition-dependent, the average values over all samples are given.

Site	Wyckoff symbol	x	y	z
A	2i	0	0	0
B	4f	0.3982(5)	0.3982(5)	0
C	8i	0.4635(4)	0.1297(5)	0
D	8i	0.7456(9)	0.0686(15)	0
E	8j	0.1819(3)	0.1819(3)	0.2469(11)

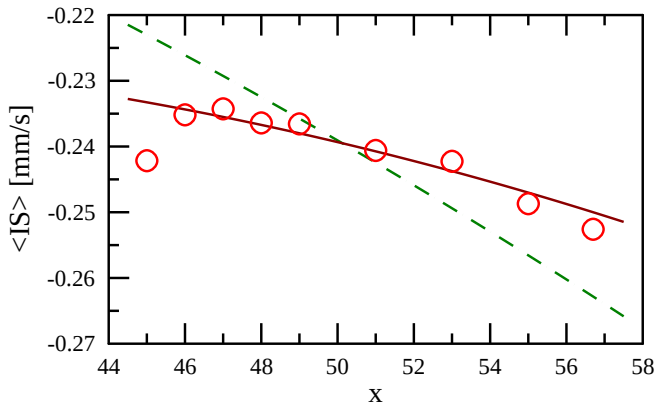

FIG. 5: (Online color) The average isomer shift (relative to the Co/Rh source), $\langle IS \rangle$, versus Mo concentration, x, as measured (circles) and as calculated (lines). The dashed line corresponds to the results obtained with approximation (1), while the solid line with approach (2).

elsewhere[16,17],

The charge-densities, ρ_e, obtained as a result of these calculations were analyzed as a function of the number of the nearest-neighbor Fe atoms, NN_{Fe}. Graphical illustrations of the $\rho_e = f(NN_{Fe})$ dependences are presented in Fig. 6. Two types of analysis were carried out. First it was assumed the ρ_e-NN_{Fe} dependence, was linear, which is best seen for the sites D and E. Taking into account probabilities of each atomic configuration considered, the $\langle IS \rangle$-values were calculated for each sublattice, and, finally, for each spectrum. The dependence of $\langle IS \rangle$ on x obtained within this approach is shown in Fig. 5 as a dashed line. Obviously, it does not agree with the values derived from the ISD-curves represented by circles in Fig. 5 which means the the linear dependence assumed in this approach was not correct. In the second approach, the average isomer shift for each subspectrum in a given spectrum was calculated as an arithmetic average over all atomic configurations considered in the calculations. The average IS for the whole spectrum was computed as a weighted average over all five sublattices (the weight of each subspectrum being its relative spectral area). The $\langle IS \rangle(x)$ dependence determined in this way is shown in Fig. 5 as a full line. It is clear that it agrees very well with the experimentally found values.

Based on the measured sublattice occupancies, calculated potentials and using the extended point charge model as outlined elsehwere[17], it was also possible to determine quadrupole splittings values, QS. As shown in Fig. 7, the QS-values are characteristic of a given lattice site, and for all of them but A, they exhibit a weak linear increase with x (for A there is a weak linear decrease). The smallest QS-value of 0.21 mm/s was found for the sublattice D, while the largest one, 0.47 mm/s, for the site E. The values of QS for the other three sites have intermediate values. Noteworthy, similar values and relations were found for the σ-phase in Fe-Cr and Fe-V systems[16,17] which is reasonable in the light of the same crystallographis structure.

The physical quantities determined in this study viz. the site occupancies, the charge-densities (isomer shifts) and the quadrupole splittings are sufficient to carry out a proper analysis of the Mössbauer spectra in terms of the five subspectra corresponding to the five sublattices. Only five free parameters were needed to successfully analyze the spectra. Four of them i.e. a background, spectral area, line width (common for all five subspectra) and the isomer shift of one of the subspectra depend on the conditions of the spectra measurements, so they cannot be calculated. The fifth free parameter was a proportionality constant between the calculated electric field gradient component, V_{zz}, and the corresponding spectral parameter viz. QS. Examples of the spectra modeled in this way together with the calculated subspectra corresponding to the particular lattice sites, are illustrated in Fig. 8. A very good quality of the fits achieved can be taken as a proof that using the electronic structure calculations (KKR-method) the determined spectral parameters adequately represent values of the hyperfine parameters characteristic of the investigated samples. In other words, a combination of the Mössbauer-effect measurements with the calculations of the electronic structure permited to properly analyze the former in terms of the spectral parameters corresponding to the different lattice sites.

IV. CONCLUSIONS

The following conclusions can be drawn based on the results reported in this paper:

1. The pure σ-phase in the Fe-Mo alloy system can be obtained between about 46 and 56.7 at% Mo.
2. Its lattice parameters a and c linearly increase with the Mo content, x.
3. The c/a ratio is concentration independent and equal to 0.52233(2).
4. The sites A and D are 100% occupied by Fe atoms, while the sites B, C and E are populated by both types of atoms.The population of Fe atoms on the latter three sites is in minority and it linearly decreases with x.
5. The average isomer shift weakly decreases with x.

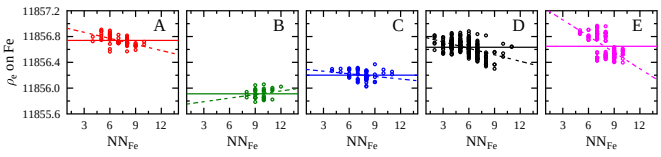

FIG. 6: (Online color) Fe-site charge density, ρ_e, for five crystallographic sites versus NN_{Fe}. Dashed lines correspond to the best linear fit to the data, whereas solid lines represent average values of ρ_e

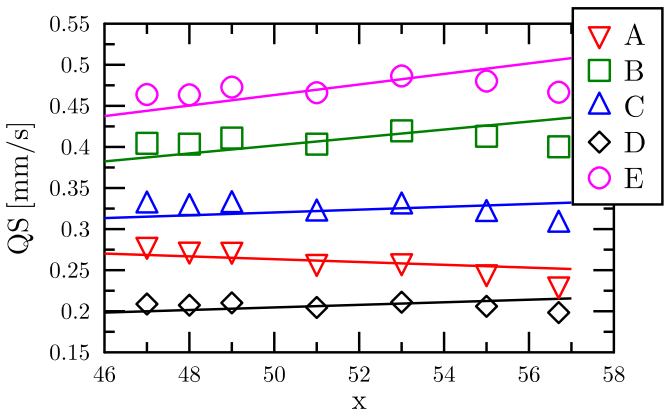

FIG. 7: (Online color) Quadrupole splitting, QS, as determined for each site and Mo concentration, x, from the analysis of the measured spectra with the protocol described in Ref. 17.

6. The calculated charge-densities are characteristic of a given sublattice; the highest one being at site D, and the lowest one at site B.

7. The calculated quadrupole splittings are characteristic of a given sublattice: the largest one being at site E, and the smallest one at site D.

Acknowledgments

The results reported in this study were obtained within the project supported by the Ministry of Science and Higher Education, Warsaw (grant No. N N202 228837).

* Corresponding author: cieslak@novell.ftj.agh.edu.pl

[1] C. Frank and J. S. Kasper, Acta Cryst. **11**, 184 (1958); ibid Acta Cryst. **12**, 4831 (1959).
[2] H.J. Goldschmidt, Research, Lond. **2**, 344 (1949).
[3] G. Bergman and D.P. Shoemaker, Acta Cryst. **7**, 857 (1954).
[4] C.G. Wilson and F.J. Spooner, Acta Cryst. **16**, 63 (1963).
[5] F.J. Spooner and C.G. Wilson, Acta Cryst. **17**, 1533 (1964).
[6] H.L. Yakel, Acta Cryst. **B39**, 28 (1983).
[7] C.P. Heijwegen and G.D. Rieck, J. Less Common Metals **37**, 115 (1974).
[8] A.F. Guillermet, Bull. of Alloy Phase Diag. **3**, 359 (1982).
[9] H. Arnfelt, Carnegie Scholarship Memoirs, Iron and Steel Inst. **17**, 6 (1928).
[10] A.K. Sinha, R.A. Buckley and W. Hume-Rothery, J. Iron and Steel Inst. **205**, 191 (1967).
[11] S.M. Dubiel and J. Cieslak, Crit. Rev. Sol. Stat. Mater. Sci. **36**, 191 (2011).
[12] J. Rodriguez-Carjaval, Phisica B **192**, 55 (1993).
[13] J.-M. Joubert Progr. Mater. Sci. **53**, 528 (2008).
[14] J. Cieslak, M. Reissner, S. M. Dubiel, J. Wernisch and W. Steiner, J. Alloys Comp. **460**, 20 (2008).
[15] J. Cieslak, S.M. Dubiel and B. Sepiol, Solid State Commun. **111**, 613 (1999)
[16] J. Cieslak, J. Tobola, and S. M. Dubiel, Phys. Rev. B **81**, 174203 (2010).
[17] J. Cieslak, J. Tobola, S. M. Dubiel, S. Kaprzyk, W. Steiner and M. Reissner, J. Phys.: Condens. Matter. **20**, 235234 (2008).
[18] ed. by, W. H. Butler, P. Dederichs, A. Gonis, and R. Weaver, *Chapter III, in: Applications of Multiple Scattering Theory to Materials Science*, vol. 253 (MRS Symposia Proceedings, MRS Pittsburgh., 1992).
[19] T. Stopa, S. Kaprzyk, and J. Tobola, J. Phys.: Condens. Matter **16**, 4921 (2004).
[20] A. Bansil, S. Kaprzyk, P. E. Mijnarends, and J. Tobola, Phys. Rev. B **60**, 13396 (1999).
[21] S. Kaprzyk, and P. E. Mijnarends, J. Phys. C **19**, 1283 (1986).

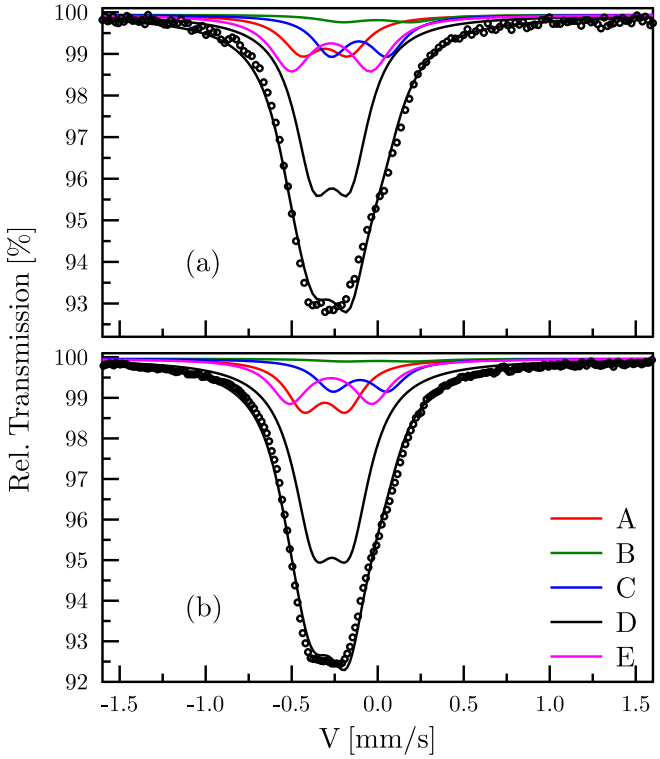

FIG. 8: (Online color) ^{57}Fe-site Mössbauer spectra recorded at 294K on two studied samples viz. with (a) $x = 48$ and (b) $x = 55$. The best-fit spectrum and five subspectra are indicated by solid lines.